Asian Journal of Chemistry; Vol. 30, No. 11 (2018), 2533-2538

ASIAN JOURNAL OF CHEMISTRY

https://doi.org/10.14233/ajchem.2018.21527

Photocatalytic Activity of Carbon Nanotubes Synthesized by Flame Fragments Deposition Method and Its Composites with TiO_2

ASMAA H. HAMMADI[1], ABBAS J. ATIYAH[2] and FALAH H. HUSSEIN[1,3,*]

[1]College of Pharmacy, University of Babylon, Hilla, Iraq
[2]Department of Chemistry, College of Science, University of Babylon, Hilla, Iraq
[3]Al-Mustaqbal University College, Babylon, Iraq

*Corresponding author: E-mail: abohasan_hilla@yahoo.com

Received: 18 June 2018; *Accepted*: 5 August 2018; *Published online*: 27 September 2018; AJC-19107

The photocatalytic activity of carbon nanotubes (CNTs) synthesized by flame fragments deposition (FFD) and CNTs/TiO_2 composites was determined by their application on the photocatalytic degradation of cobalamin dye. Different ratios of composites consisting of carbon nanotubes with titanium dioxide nanoparticles anatase were prepared using a simple, low temperature process in which carbon nanotubes and anatase nanoparticles were dispersed in water. The ratios that used in the present work were, 25:1, 50:1, 75:1 and 100:1 from theTiO_2 (30 nm)/CNTs. The structures of different TiO_2/CNT composites were characterized by Raman spectroscopy, X-ray diffraction, FTIR spectroscopy and atomic force microscopy. The photocatalytic activity of these materials was investigated by following the photocatalytic removal of cobalamin dye over these prepared materials. The obtained results showed an increment in the efficiency of cobalamin dye removal over TiO_2/CNTs composites in comparison with neat components TiO_2 and carbon nanotubes under the same reaction condition. The photocatalytic removal of cobalamin dye from aqueous solution over TiO_2/CNTs composites was followed spectrophotometrically by measuring absorbance of the dye solution at 550 nm. The efficiency of cobalamin dye removal over neat components and composites falls in the following order: 50:1 > 75:1 > 100:1 > 25:1 > CNTs > TiO_2.

Keywords: Photocatalytic activity, Carbon nanotubes, Titanium dioxide nanoparticles, Cobalamin dye, Adsorption.

INTRODUCTION

Carbon nanotube is rolled up from one or more graphene sheets concentrically [1]. Depending on the number of graphite layers, carbon nanotubes are classified as single-wall carbon nanotubes (SWCNTs), double-wall carbon nanotubes (DWCNTs) or multi-wall carbon nanotubes (MWCNTs) [2]. Single-wall carbon nanotubes (SWNTs) are a unique class of material that have received an enormous amount of attention over recent years, because of their remarkable mechanical, thermal, electronic and optical properties [3,4]. Syntheses of carbon nanotubes by several methods includes arc discharge, laser ablation and chemical vapor deposition [5], yielding tubes of various diameter and length distributions [6].

Carbon nanotubes are sub-atomic scale containers of graphitic carbons with remarkable electronic, mechanical and warm properties [7]. The synergistic impact of carbon nanotubes on the action of composite impetus can be clarified as far as its activity as adsorbents and a scattering agent. The advance CNTs conductive structure may encourage the division of the photograph created electron/gap sets at the TiO_2-CNT interface prompting the quicker rates of photocatalytic oxidation and improvement in the proficiency of titanium dioxide [8].

Different techniques have been utilized for the planning of TiO_2-CNTs composites. For the most part, TiO_2 is covered on the surface of the carbon nanotube. The composites can be set up by different methods which incorporate sol-gel, impregnation, electro-turning, electrophoretic statement, compound vapor testimony and aqueous method [9-11]. TiO_2-CNTs composite material have been appearing to expand the rodent of photograph reactant oxidation of toxins [12]. The conductivity structure of carbon nanotube platforms may encourage the detachment of the photograph created (e-h) pairs at TiO_2-CNTs interface prompting the quicker rates of photograph synergist oxidation [13].

Different applications and difficulties for these composite materials are accounted for carbon nanotube-anatase titanium dioxide CNT/TiO_2 composite [14]. Recently, CNTs/TiO_2 composites have been attracting much care because of their excellent properties, including electrical properties, chemical and thermal stability, high adsorption capacity and high aspect ratio [8,15,16]. The applications of TiO_2/CNTs composites for the big problem of pollutions obligation to their highest capability to behavior electrons and adsorb hydrophobic organic pollutants, barely adsorbed by TiO_2 nanoparticles themselves [15]. In this paper, we reported the photoactivity of CNTs/TiO_2 anatase (nanopar-ticle) composite on removal of cobalamin (m.f. $C_{63}H_{88}N_{14}PCo$) and compared the adsorption capacity of TiO_2, CNTs and CNTs/TiO_2 composite.

EXPERIMENTAL

Cobalamin dye (m.f. $C_{63}H_{88}N_{14}PCo$) was purchased from Sigma having purity < 98.5 %. Titanium dioxide nanoparticles (TiO_2) anatase (10-30 nm) purities 99 % from Sky Spring Nanomaterials Inc. Acetone from S.D. Fine-Chem. Ltd., India with purities 99 % and hydrogen peroxide was purchased from Barcelona, Spain in 30 % by weight. The N_2 gas used in purities 99.999% from Emirates industrial gases.

Synthesis of carbon nanotubes: In this part, carbon nanotubes (CNTs) were synthesized according to flame fragments deposition method using a homemade chamber instrument constructed for synthesized of carbon nanotubes (CNTs) from Iraqi natural gas as carbon source. The instrument consists of nine collection centers at the top position where is embedded in each position. One of them is used without catalyst and the other eight with different types of catalysts. Rümmeli *et al.* [17] synthesized of carbon nanotubes without catalysts and with catalysts (Fe^{2+}:Mo:Mg). The catalysts (Fe^{2+}:Mo:Mg) ratio (1:0.1:11). The catalyst was prepared by using combustion methods as in the literature [18]. An aqueous solution consisting of $FeSO_4$ and ammonium molybdate $(NH_4)_6{\cdot}Mo_7{\cdot}O_{24}{\cdot}4H_2O$ were mixed together with a weight ratio of Fe:Mo equal to 1:0.1 and with stirring for 1 h. The bimetallic solution was introduced to $Mg(NO_3)_2{\cdot}6H_2O$ solution and 1 g of citric acid with a weight ratio of Fe:Mg:Mo equal to 1:11:0.1, respectively, followed by sonication for 1 h. The solution was stirred for 10 h with an increase in temperature to 60 ºC in order to dry the mixture. The powder was treated thermally at 150 ºC for 10 h in nitrogen atmosphere by using tube furnaces and then ground in a mortar to remove any agglomerate that may have formed during the final composition of the trimettalic catalyst. After the crucibles were fogged by catalyst, synthesized of carbon nanotubes.The carbon nanotubes were characterized using the X-ray diffraction (XRD) and Raman analysis.

Purification of carbon nanotubes: The purification of synthesized carbon nanotubes was peformed *via* oxidation with H_2O_2 then treated with acetone using separation funnel. Carbon nanotubes (100 mg) was dispersed in 50 mL of H_2O_2 and sonicated for 1 h. The mixture was left in the refrigerator at 4 ºC for 24 h, after that the solution allowed to reach room temperature, then heated gradually to 50 ºC until all hydrogen peroxide removed completely. Finally, the sample was washed with deionized water and dried at 80 ºC for 4 h. After that addition of 15 mL acetone to the dry sample and sonicated for 15 min. The suspension was then centrifuged for 15 min. The separated carbon nanotubes were then calcined at 275 ºC for 2 h and finally characterized using X-ray diffraction (XRD) and Raman spectroscopy.

Functionalization of carbon nanotubes: Functionalization of carbon nanotubes is an important step that can be used in order to introduce some functional groups into the surface and improve its surface properties. In this context, carbon nanotubes (100 mg) were suspended in 75 mL H_2O_2 (30 % weight) in a 100 mL round bottom flask equipped with a condenser and the dispersion was heated to 80 ºC at reflux for overnight.

After the reflux, the suspension containing carbon nanotubes and H_2O_2 was heated to 50 ºC with irradiation under an (UV) lamp for 5 h to dry the mixture. The oxidation of carbon nanotubes surface is very important to produce the composite. The homogeneous diffusion of O-CNTs takes place in distilled water due to formation of hydrogen bonding. They formed functioned O-CNTs was investigated using FTIR.

Synthesis TiO_2/CNTs composites: Different ratios from titanium dioxide nanoparticles (TiO_2) anatase/CNTs composite structures were prepared by a simple evaporation and drying process. To prepare TiO_2/CNTs composite, approximately10 mg carbon nanotubes was dispersed in 150 mL of distilled water and sonicated for 15 min, titanium dioxide powder was added to the carbon nanotubes suspension with continuous stirring. After that it was sonicated for 10 min, the suspension containing carbon nanotubes and TiO_2 particles was heated to 80 ºC with flushing O_2 gas in solution to accelerate the evaporation of water. Then, the composite was dried overnight in an oven at 104 ºC to avoid oxidation of the carbon nanotubes. Different composites were prepared using different ratios of TiO_2 (30 nm) and carbon nanotubes. These mass ratios were 25:1, 50:1, 75:1 and 100:1. The obtained composites were investigated using (XRD) and atomic force microscopy (AFM).

Activity of pristine TiO_2, carbon nanotubes and anatase TiO_2: The photocatalytic activity of pristine CNTs and TiO_2 and composites of different ratios 25:1, 50:1, 75:1 and 100:1 to form TiO_2/CNTs was investigated by following the decolorization of cobalamin dye in an aqueous solution of 100 mL (40 ppm) under UV light. Aqueous suspensions of CNT and/or TiO_2 containing cobalamin dye in a beaker under continuous stirring under irradiation with UV light at wavelength of 365 nm. The required amount of the catalyst was suspended in 100 mL of aqueous solution of cobalamin. After illumination, 2 mL was taken from the reaction suspension, centrifuged at 6000 rpm for 15 min and then filtered to remove the particles. The second centrifugation was found necessary to remove fine particles of carbon nanotubes, TiO_2, 25:1, 50:1, 75:1 and 100:1 from TiO_2 (30 nm)/CNTs. The absorbance of cobalamin was then determined at 550 nm.

RESULTS AND DISCUSSION

Activity of CNTs/TiO_2 composite: The photocatalytic activity of both neat of TiO_2, CNTs and the synthesized composites was investigated by following the photocatalytic removal of cobalamin dye (40 ppm) from aqueous solutions under irradiation with UV light. Fig. 1 shows the changes in removal

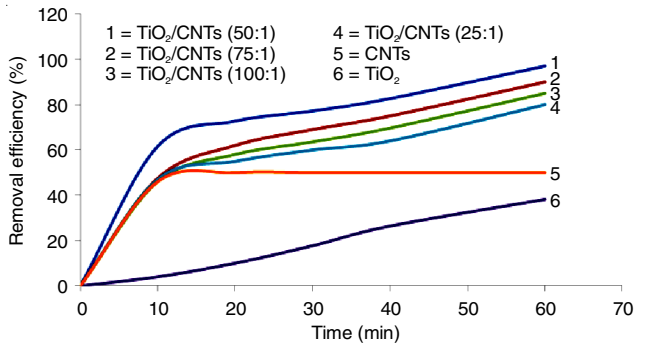

Fig. 1. Effect of time of adsorption on the removal efficiency of CA dye (40 ppm) over neat TiO_2, CNTs and TiO_2/CNTs composites

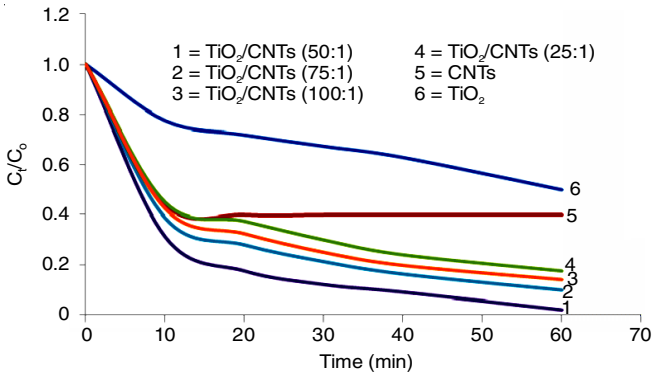

Fig. 2. Effect of time of adsorption on the relative concentration of cobalamin dye

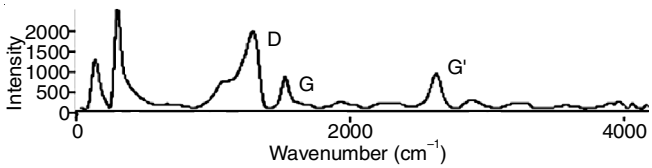

Fig. 3. Raman spectroscopy for CNTs after purification

efficiency of the cobalamin dye in aqueous solution upon irradiation over CNTs/TiO_2 composite in different ratios. The results indicate that carbon nanotubes can enhance adsorption properties of TiO_2 anatase due to increase surface area of produced composites in comparison with neat components of used composites [19]. The obtained results are presented in Fig. 1.

The optimum removal efficiency was achieved with composite (50:1) around 97 %. The efficiency of photocatalytic degradation of cobalamin dye over other composites of TiO_2/ CNTs ratios (75:1, 100:1, 25:1) and neat CNTs and TiO_2 were around 90, 86, 80, 50 and 38 %, respectively. In general, the efficiency of dye removal over the used composites were more efficient than neat TiO_2 and CNTs which indicated that all ratios of TiO_2/ CNTs composites lead to enhance surface properties with increasing of specific surface area of the prepared composites. This can lead to improve catalytic activity of all the composites in comparison of neat components which leads to the separation of photogenerated electron-hole pairs and decrease of their recombination rate and thus display significantly enhanced photocatalytic activity for removal of cobalamin dye in aqueous solution under UV irradiation.

The results of cobalamin dye removal by adsorption onto different photocatalysts are presented in Fig. 2. From these results, it can be seen that there is a progressive increment in the efficiency of dye removal with time progressing. Besides that composites are more efficient than separated components in dye removal under the same adsorption conditions. For composite of TiO_2/CNTs equilibrium adsorption is being achieved within 0.5 h for four prepared ratios of TiO_2/CNTs composites. When adsorption reaches equilibrium the efficiency of cobalamin adsorption onto composites and neat components fall in the following order: 50:1 > 75:1 > 100:1 > 25:1 > CNTs > TiO_2. This result can be attributed to the improvement of catalytic properties and increment of specific surface area of the prepared composites in comparison with their single components. The carbon nanotubes can increase surface area for synthesized composites and then reduce the rate of electron-hole recombination on TiO_2 by injecting conduction band electrons into to the surface of carbon nanotubes leading to reduced back electron transfer. This can lead to improve the total efficiency of photocatalytic activity of decolorization of cobalamin dye over the used composites.

Characterization of TiO_2, CNTs and TiO_2/CNTs composites: Fig. 3 shows the Raman spectra for carbon nanotubes. Three bands are observed at 1341 cm^{-1} (D), 1581 cm^{-1} (G) and 2700 cm^{-1} (G′). The peak at 1341 cm^{-1} in the spectrum for carbon nanotubes compare to D-band of confused graphitic carbon in carbon nanotubes. The peak at 1581 cm^{-1} in the spectrum for carbon nanotubes relates to G-band of graphitic carbon in carbon nanotubes while D- and G-groups show the nearness of crystalline graphite carbon in carbon nanotubes. The G′ band at 2700 cm^{-1} are sensitive to the freight exchanged between the nanotubes and the demote moiety [20].

Crystal structure of carbon nanotubes was investigated using XRD patterns using (Rigaku Rotalflex) (RU-200B) X-ray diffractometer with CuKα radiation (λ = 0.15405 nm) with a Ni filter. The tube current was 100 mA with a tube voltage of 40 kV. XRD patterns were performed in range of 2θ between 10º and 80º with a scan rate of 5º/min with a resolution in the 2θ scans was at 0.02º. XRD patterns for the synthesized carbon nanotubes are shown in Fig. 4, which shows the characteristic peaks at 24.56º and 44.16º, these peaks are related to carbon nanotubes after purification. These results indicate that carbon nanotubes synthesized by flame fragments deposition are in good quality compared with that obtained by using chemical vapour deposition techniques [21].

The FTIR analysis was performed to confirm the presence of the introduced functional groups into the surface of CNTs

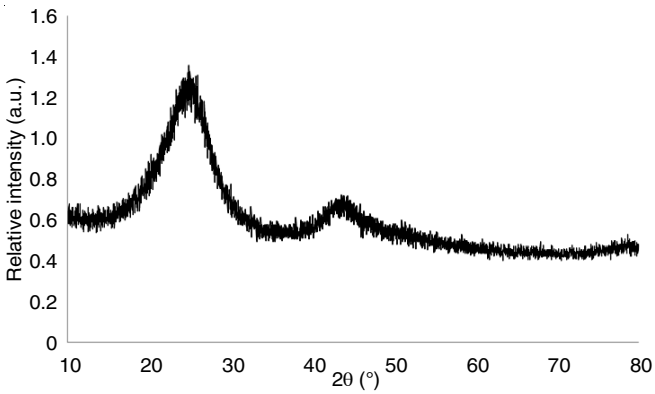

Fig. 4. XRD patterns for the synthesized CNTs

after functionalization processes. Oxidation of CNTs with H_2O_2 (30 % weight) and UV-irradiation introduces some functional groups like-OH and-COOH. These surface groups are supportive to form interaction and chemical bonding between CNTs and TiO_2 [22]. FTIR spectra of functionalized CNTs exhibits characteristic strong and broad bands between 3600-3173 cm^{-1}, which can be assigned to O-H stretching vibrations in C-OH groups. The band between 1760-1690 cm^{-1} is related to C=O stretching vibrations in carboxyl groups (Fig. 5) [23].

The surface morphology of synthesized CNTs was investigated using atomic force microscope (AFM). The obtained AFM images show filaments with length 1-1.5 μm and diameter around 0.5 μm, which appeared as bundles in TiO_2/CNTs composite (ratio 50:1) filaments (Fig. 6). The CNTs bundles easily bend and wrap around anatase TiO_2 particles, because of the weak van der Waals interaction between the CNTs in bundles [24].

The CNTs bundles which appear to be about 40 nm in diameter (Fig. 7a) while TiO_2 particles show a diameter around 50 nm (Fig. 7b). The TiO_2/CNTs composite with a ratio of 25:1 is lesser than different ratios 50:1 ,75:1 and 100:1 because of the large CNTs amount concludes that light did not reach to all particles (Fig. 7c) while the TiO_2/CNTs composite with a ratio of 50:1 is greater than different ratios 25:1 ,75:1 and 100:1 might be due to the large diameter 50 nm (Fig. 7d). The ratios of 75:1 and 100:1 are lesser than ratio 50:1, so the surface area is reduced due to increased TiO_2 amount (Fig 7e-f).

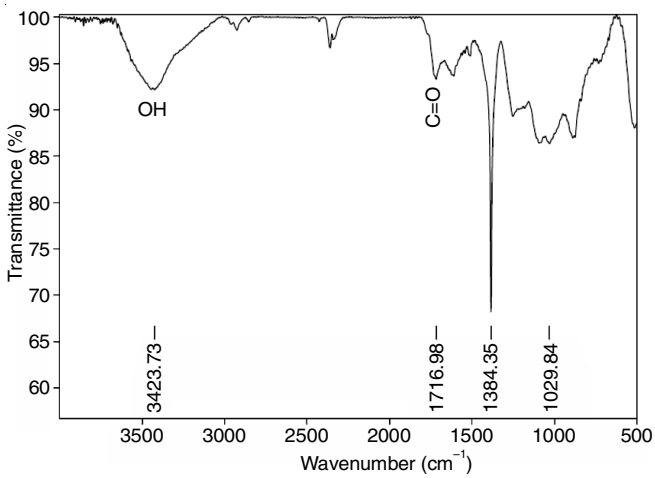

Fig. 5. FTIR spectra for functionalization of carbon nanotubes

Fig. 8 shows the XRD patterns of CNTs, TiO_2 and CNTs/TiO_2 composite. The most intense peaks of CNTs agreed to the 24.56º (002) reflection and 43.16º (100) band, the peaks for TiO_2 are 25.33º (101), 37.88º (004), 47.68º (200), 54.14º (105),

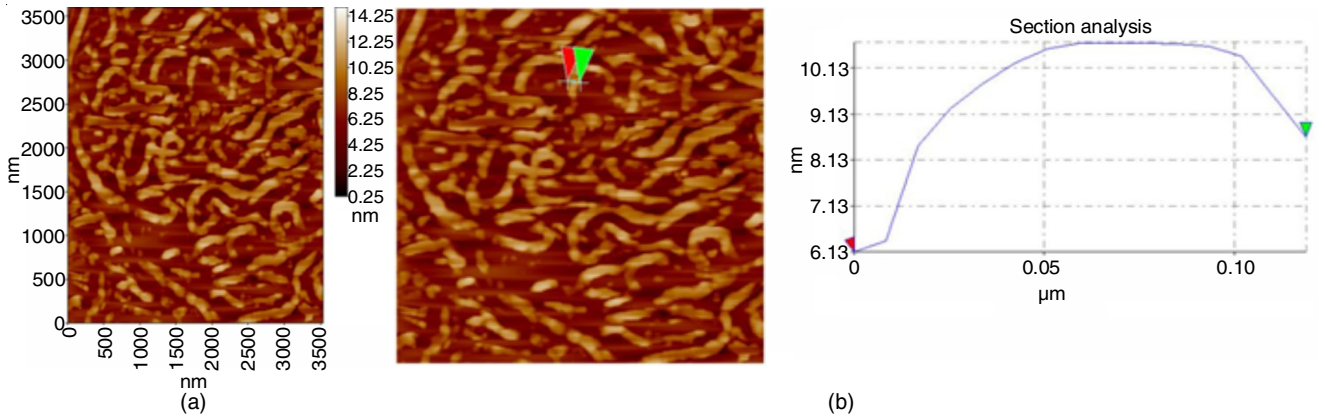

Fig. 6. AFM for synthesized CNTs

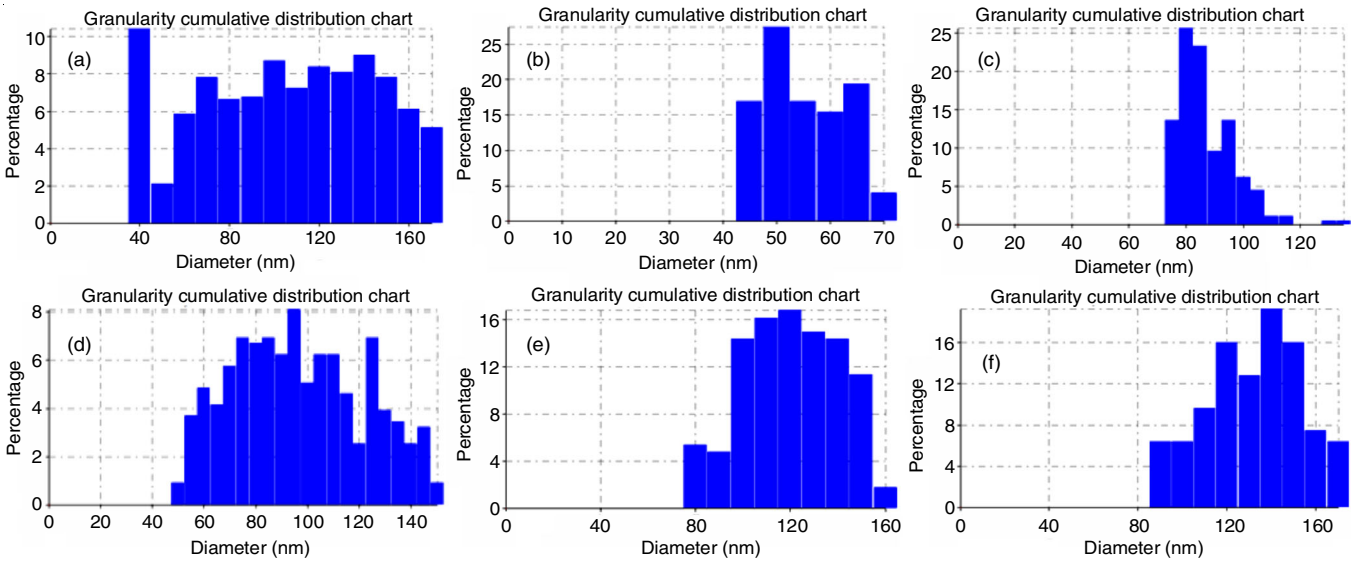

Fig. 7. Granularity cumulation distribution for (a) CNTs, (b) TiO_2 and (c-f) different ratio of TiO_2/CNTs composites, C (25:1), d (50:1), e (75:1), f (100:1)

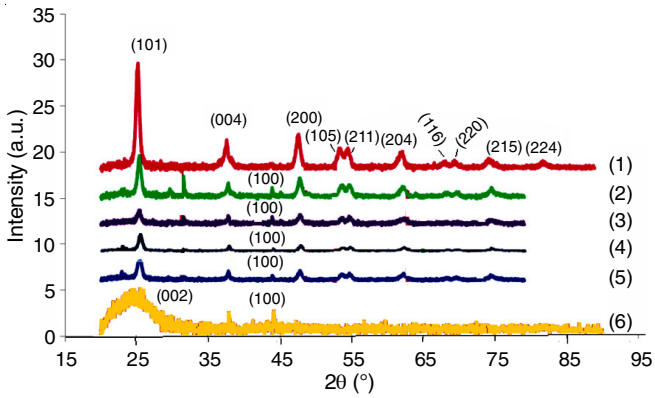

Fig. 8. XRD patterns for synthesized (6) CNTs, (1) TiO_2 and (2-5) different ratio of TiO_2/CNTs composites

54.91º (211), 62.50º (204), 70.00º (116), 70.89º (220) 75.16º (301). The additional peaks present in all the diffractograms agree to the TiO_2 form of TiO_2. The peak at 24.56º (002) reflection due to CNTs intersections in the TiO_2 25.33º (101) reflection. It is worth to notice that the intensity of TiO_2 diffraction peaks increases from sample (1 to 5) and the width at half height of the peaks decreases. This is consistent with the increasing amount of TiO_2 from samples 2 to 5, which gives more stretched crystallized areas on the surface. The composite shows all these above points out peaks promotes the formation of TiO_2/CNTs composite.

Mechanism of enhancement of photocatalysis of CA dye over CNTs/TiO_2 composite: Mechanism for removal of cobalamin dye over CNTs/TiO_2 composite and neat components of each of TiO_2 and CNTs are shown in Fig. 9. Upon light irradiation of composite photocatalyst conduction band electron (CB^-) and valence band hole (VB^+) pairs can be produced. It is believed that carbon nanotub can behave as an electron entrapment and part of photo-produced electrons in CB^- of TiO_2 are rapidly can be injected to carbon nanotubs and the photogenerated charge carriers under these circumstances are excellently separated as explained in the following equations:

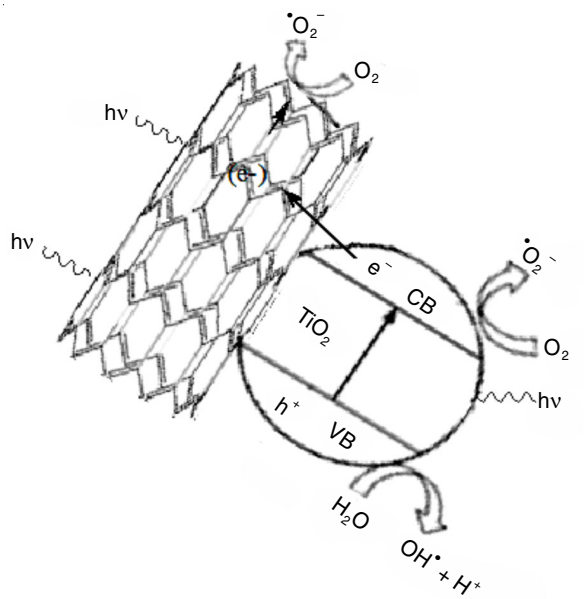

Fig. 9. Schematic description of a proposed model for the CNT/TiO_2 working mechanism

$$CNT/TiO_2 + h^+ \longrightarrow CNT/TiO_2\ (e^- + h^+) \quad (1)$$

$$CNT/TiO_2\ (e^- + h^+) \longrightarrow CNT\ (e^-) + TiO_2\ (h^+) \quad (2)$$

$$CNT\ (e^-) + O_2 \longrightarrow CNT + O_2^{\bullet-} \quad (3)$$

$$TiO_2\ (h^+) + H_2O \longrightarrow TiO_2 + OH^\bullet \quad (4)$$

$$O_2^{\bullet-} + OH^\bullet + \text{Cobalamin dye} \longrightarrow \text{Intermediate products} \longrightarrow CO_2 + H_2O \quad (5)$$

They produced highly reactive $O_2^{\bullet-}$ and $OH^\bullet$ radicals degrade the cobalamin dye to form several intermediates and finally the formed intermediates into CO_2 and H_2O.

Conclusion

Titanium dioxide nanoparticles (TiO_2) anatase/CNTs composite photocatalysts with different ratios were prepared by a simple evaporation and drying process. The TiO_2/ CNTs (50:1) composite had higher activity of about four different ratios of TiO_2/ CNTs composites, TiO_2 and CNTs. The CNTs with TiO_2 had characterized the key of high efficiency for decolorization for cobalamin dye. The results indicate that the decolorzation efficiency percentage of cobalamin dye with TiO_2/ CNTs composite was higher that titanium dioxide or CNTs. The efficiency of color removed increase with time. The removal efficiency of cobalamin was found to be 97 %. The results show that the photocatalytic activity of different ratios in this study was 50:1 > 75:1 > 100:1 > 25:1 > CNTs > TiO_2. This result can be attributed due to the improvement of catalytic properties and increment of specific surface area of the prepared composites in comparison with their single components.The carbon nanotubes can increase surface area for synthesized composites and then reduce the rate of (e-h) recombination on TiO_2.

CONFLICT OF INTEREST

The authors declare that there is no conflict of interests regarding the publication of this article.

REFERENCES

1. A. Aqel, K.M.M.A. El-Nour, R.A.A. Ammar and A. Al-Warthan, *Arab. J. Chem.*, **5**, 1 (2012); https://doi.org/10.1016/j.arabjc.2010.08.022.
2. C. Liu and H.-M. Cheng, *Mater. Today*, **16**, 19 (2013); https://doi.org/10.1016/j.mattod.2013.01.019.
3. E. Del Canto, K. Flavin, D. Movia, C. Navio, C. Bittencourt and S. Giordani, *Chem. Mater.*, **23**, 67 (2011); https://doi.org/10.1021/cm101978m.
4. P. Mahalingam, B. Parasuram, T. Maiyalagan and S. Sundaram, *J. Environ. Nanotechnol.*, **1**, 53 (2012).
5. V.N. Popov, *Mater. Sci. Eng.*, **43**, 61 (2004); https://doi.org/10.1016/j.mser.2003.10.001.
6. T.-J. Park, S. Banerjee, T. Hemraj-Benny and S.S. Wong, *J. Mater. Chem.*, **16**, 141 (2006); https://doi.org/10.1039/B510858F.
7. G. Hu, X. Meng, X. Feng, Y. Ding, S. Zhang and M. Yang, *J. Mater. Sci.*, **42**, 7162 (2007); https://doi.org/10.1007/s10853-007-1609-7.
8. K.D. Shitole, R.K. Nainani and P. Thakur, *Def. Sci. J.*, **63**, 435 (2013); https://doi.org/10.14429/dsj.63.4870.
9. H. Chen, S. Yang, K. Yu, Y. Ju and C. Sun, *J. Phys. Chem.*, **115**, 3034 (2011); https://doi.org/10.1021/jp109948n.
10. N. Bouazza, M. Ouzzine, M.A. Lillo-Rodenas, D. Eder and A. Linares-Solano, *Appl. Catal. B*, **92**, 377 (2009); https://doi.org/10.1016/j.apcatb.2009.08.017.

11. R. Leary and A. Westwood, *Carbon*, **49**, 741 (2011); https://doi.org/10.1016/j.carbon.2010.10.010.
12. W. Wang, P. Serp, P. Kalck, C.G. Silva and J.L. Faria, *Mater. Res. Bull.*, **43**, 958 (2008); https://doi.org/10.1016/j.materresbull.2007.04.032.
13. M.-L. Chen, F.-J. Zhang and W.-C. Oh, *New Carbon Mater.*, **24**, 159 (2009); https://doi.org/10.1016/S1872-5805(08)60045-1.
14. K. Woan, G. Pyrgiotakis and W. Sigmund, *Adv. Mater.*, **21**, 2233 (2009); https://doi.org/10.1002/adma.200802738.
15. M. Alsawat, T. Altalhi, K. Gulati, A. Santos and D. Losic, *ACS Appl. Mater. Interfaces*, **7**, 28361 (2015); https://doi.org/10.1021/acsami.5b08956.
16. J. Safari and S. Gandomi-Ravandi, *J. Mol. Struct.*, **1065-1066**, 241 (2014); https://doi.org/10.1016/j.molstruc.2014.02.035.
17. M.H. Rümmeli, A. Bachmatiuk, F. Börrnert, F. Schäffel, I. Ibrahim, K. Cendrowski, G. Simha-Martynkova, D. Plachá, E. Borowiak-Palen, G. Cuniberti and B. Büchner, *Nanoscale Res. Lett.*, **6**, 303 (2011); https://doi.org/10.1186/1556-276X-6-303.
18. B. Liu, S. Lyu, S. Jung, H. Kang, C. Yang, J. Park, C. Park and C. Lee, *Chem. Phys. Lett.*, **383**, 104 (2004); https://doi.org/10.1016/j.cplett.2003.10.134.
19. A.M. Kamil, F.H. Hussein, A.F. Halbus and D.W. Bahnemann, *Int. J. Photoenergy*, **Article ID 475713** (2014); https://doi.org/10.1155/2014/475713.
20. M. Ahmed, H.M.N. Iqbal and Z. Akram, *Arab. J. Sci. Eng.*, **43**, 23 (2018); https://doi.org/10.1007/s13369-017-2662-4.
21. A.M. Jassm, F.H. Hussein, F.H. Abdulrazzak, A.F. Alkaim and B.A. Joda, *Asian J. Chem.*, **29**, 2804 (2017); https://doi.org/10.14233/ajchem.2017.20994.
22. B. Czech, P. Oleszczuk and A. Wiacek, *Environ. Pollut.*, **200**, 161 (2015); https://doi.org/10.1016/j.envpol.2015.02.020.
23. N.I. Kovtyukhova, T.E. Mallouk, L. Pan and E.C.J. Dickey, *J. Am. Chem. Soc.*, **125**, 9761 (2003); https://doi.org/10.1021/ja0344516.
24. Y. Yao, G. Li, S. Ciston, R.M. Lueptow and K.A. Gray, *Sci. Technol.*, **42**, 4952 (2008); https://doi.org/10.1021/es800191n.